

Full Paper

Ni/Al LDH Nanoparticles Modified Carbon Paste Electrode: Application to Electro-Catalytic Oxidation of Methanol

Ghasem Karim-Nezhad*, Sara Pashazadeh and Ali Pashazadeh

Department of Chemistry, Payame Noor University, PO BOX 19395-3697 Tehran, Iran

*Corresponding Author, Tel: +98 461 2349868, Fax: +98 461 2332556

E-Mail: g.knezhad@gmail.com

Received: 20 June 2012 / Accepted: 14 August 2012 / Published online: 27 August 2012

Abstract- Ni/Al Layered double hydroxide nanoparticles modified carbon paste (Ni/Al-LDH/NMCP) electrode was prepared as a new electrode. The Ni/Al-LDH/NMCP electrode was prepared by grinding the mixture of graphite powder and silicon oil (as a binder) with sufficient amount of Ni/Al Layered double hydroxide. Then, the electrode was placed in 0.1 M NaOH and the electrode potential was cycled between 0 and 700 mV (*vs.* Ag/AgCl) at a scan rate of 50 mVs⁻¹ for 20 cycles in a cyclic voltammetry regime until a stable voltammogram was obtained. Electrocatalytic activity of the modified electrode was used for the oxidation of methanol, in aqueous alkaline solution. Results showed that, the electrocatalytic activity of the Ni/Al-LDH/NMCP electrode is much higher than those of unmodified carbon paste electrode under similar experimental conditions, showing the possibility of attaining good electrocatalytic anodes for fuel cells. Kinetic parameters such as the electron transfer coefficient (α) and the number of electrons involved in the rate-determining step (n_a) for the oxidation of methanol were determined utilizing cyclic voltammetry (CV). The modified electrode shows stable and linear responses in the concentration range of 0.01 to 0.1 mol L⁻¹.

Keywords- Ni/Al Layered Double Hydroxide, Modified Carbon Paste Electrode, Electrocatalytic Oxidation, Methanol, Kinetic

1. INTRODUCTION

Fuel cells are being considered as an important technology that can be used for various power applications [1]. The electrochemical oxidation of small organic molecules is an interesting research topic on direct fuel cell. Methanol is the one being most intensively investigated among various small organic molecules [2]. Direct methanol fuel cells (DMFCs) are attractive power sources for portable electronics thanks to the advantage of low operating temperature, easy transportation and fuel storage, high-energy efficiency, low exhaustion and fast start-up [3]. In direct methanol fuel cells (DMFCs), methanol is used as a fuel and a great deal of interest exists in the development of materials with capability for the electrocatalytic oxidation of methanol [1]. Methanol as fuel has numerous advantages such as simple operation and ease of fuel storage and distribution. However, compared to the hydrogen based fuel cells, DMFC still remains to be further developed. One of the problems still unsolved is the slow kinetics of methanol oxidation on the fuel cell's anode [4].

The mechanism and kinetics of methanol oxidation have been studied under a wide range of conditions and on various electrodes including Pt [5], binary and ternary alloys [6, 7], modified electrodes [8, 9], nano-composites [10, 11] and nickel [12–14]. The most important advantage of alkaline DMFCs is the potential use of non-Pt catalysts in the electrodes, widening the range of options for materials support and catalyst. Several Pt alternative materials such as Au [15, 16] and Pd [17] have been investigated for methanol oxidation in alkaline solutions. An overview of catalysts for DMFCs can be seen in the literature [18]. Among non-Pt catalysts used for methanol electro-oxidation, nickel compounds have become more attractive in recent years because they exhibit good electrocatalytic activity for methanol oxidation in alkaline media. Therefore, many Ni-base catalysts, such as pure nickel [19, 20], nickel alloy [21–23], nickel hydroxide [24] and nickel complex [25–28], have been successfully performed to fabricate new anode and cathode catalyst systems.

Recently layered double hydroxides (LDHs) have been proposed as catalysts for the development of modified electrodes [29]. The structure of LDHs consists of positively charged brucite-like layers, whose net charge is compensated by anions located in the interlayers, which can be easily exchanged. For this reason these compounds are also called anionic clays [30]. More recently, non-electroactive Mg-Al LDH significantly enhanced the catalytic activity of Au nanoparticles (AuNPs) for the oxidation of methanol in alkaline media [31]. Wang and et al have reported Ni-Al LDH film modified GC electrode for electrocatalytic oxidation of methanol [32].

In this work, we have reported a new electrode by the use of carbon paste and Ni/Al LDH nanoparticles as substrate and modifier respectively and explored the electrocatalytic activity of the prepared electrode toward the oxidation of methanol.

2. EXPERIMENTAL

2.1. Reagents and instrumentation

Methanol and other reagents were of analytical grade supplied by Merck (Darmstadt, Germany) and were used without further purification. All solutions were prepared with doubly distilled water. Electrochemical measurements were carried out in a conventional three-electrode cell powered by an electrochemical system comprising an AUTOLAB system with PGSTAT12 boards (Eco Chemie, Utrecht, and The Netherlands). The system was run on a PC using GPES 4.9 software. A platinum wire was employed as counter electrode and an Ag/AgCl electrode served as the reference electrode.

All experiments were performed at room temperature of 25 ± 2 °C.

2.2. Preparation of Ni/Al LDH nanoparticles

The Ni/Al LDHs nanoparticles were prepared by hydrothermal method. A series of Ni/Al LDHs with nominal $\text{Ni}^{2+}/\text{Al}^{3+}$ atomic ratio of 3/1 were prepared by hydrothermal reaction at 180°C. All of them were prepared as follows: appropriate amounts of $\text{NiSO}_4 \cdot 6\text{H}_2\text{O}$ and $\text{Al}_2(\text{SO}_4)_3 \cdot 18\text{H}_2\text{O}$ ($\text{Ni}^{2+}/\text{Al}^{3+}=3/1$ (molar ratio)) were dissolved in deionized water (40 mL). Then aqueous solution of $0.5 \text{ mol L}^{-1} \text{Na}_2\text{CO}_3$ and $3 \text{ mol L}^{-1} \text{NaOH}$ was added to the above solution drop by drop with vigorous stirring to adjust the pH value of the solution. After that, the suspension was transferred into a 50 mL stainless Teflon-lined autoclave and heated at 180°C for appropriate time, then cooled to room temperature naturally. The resulting products were filtrated and washed several times with distilled water and absolute ethanol. The apple-green solid was then collected and dried at room temperature for 12 h [33]. Nanoparticles of Ni/Al LDH were obtained.

2.3. Preparation of Ni/Al-LDH/NMCP electrode

The Ni/Al-LDH/NMCP electrode was prepared by homogenizing the 0.2 g mixture of graphite powder and Ni-Al LDH powder at a ratio of 75:25 along with 3 drops of paraffin (as a binder). The resulting paste was then packed into a polyethylene tube. The electrode surface was renewed by extrusion of approximately 0.5 mm carbon paste from the holder and smoothed using filter paper. Then, the electrode was placed in 0.1 M NaOH and the electrode potential was cycled between 0 and 700 mV (vs. Ag/AgCl) at a scan rate of 50 mV s^{-1} for 20 cycles in a cyclic voltammetry regime until a stable voltammogram was obtained. The bare carbon paste electrode was constructed by the same procedure without adding Ni-Al LDH to graphite powder. Electric contacts were made by a copper wire through the back of the electrodes. The electrode was rinsed with distilled water, and applied for electrochemical studies.

3. RESULTS AND DISCUSSION

In this study, Ni-Al LDH modified carbon paste electrode was prepared as a new electrode. For the activation of this electrode, the electrode was placed in 0.1 mol L⁻¹ NaOH and the electrode potential was cycled between 0 and 700 mV (vs. Ag/AgCl) at a scan rate of 50 mV s⁻¹ for 20 cycles in a cyclic voltammetry regime until a stable

Voltammogram was obtained (Fig. 1). As this figure shows, with increase of the scan number, the currents for both anodic and cathodic peaks increase steadily for up to 20 runs. After 20 runs, the Ni/Al-LDH/NMCP electrode shows reproducible cyclic voltammograms. A single and well-defined redox couple has found.

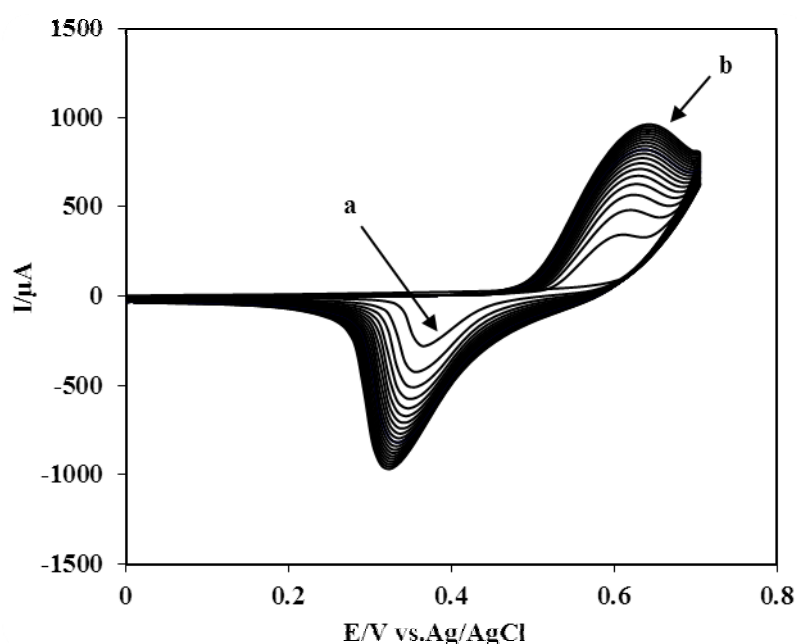


Fig. 1. Repetitive cyclic voltammograms of Ni/Al-LDH/NMCP electrode in 0.1 mol L⁻¹ NaOH in the potential range of 0 to 700 mV. Potential sweep rate is 50 mV s⁻¹. (a) First cycle and (b) end cycle

Next the cyclic voltammograms of the modified electrode were recorded in 0.1 mol L⁻¹ NaOH at various potential sweep rates (Fig. 2A). A pair of redox peaks was observed which correspond to the conversion between different oxidation states of Ni according to the equation 1.

With the increase of the scan rate, the redox current increased, the anodic peak shifted toward positive potential and overlapped with the oxygen evolution peak, and the cathodic peak shifted toward negative potential. The peak's currents (I_{pa} and I_{pc}) are proportional to sweep rates in the range of 5-100 mV s⁻¹ (Fig. 2B), pointing to the electrochemical activity of

the surface redox couple. From the slope of anodic peak currents versus scan rate, and using [34]:

$$I_p = \left(\frac{n^2 F^2}{4RT} \right) v A \Gamma^* \quad (1)$$

Where v is the sweep rate, A is the geometric surface area and Γ^* is the surface coverage of the redox species, the calculated value of Γ^* can be approximately $9.55 \times 10^{-5} \text{ mol cm}^{-2}$ for $n=1$.

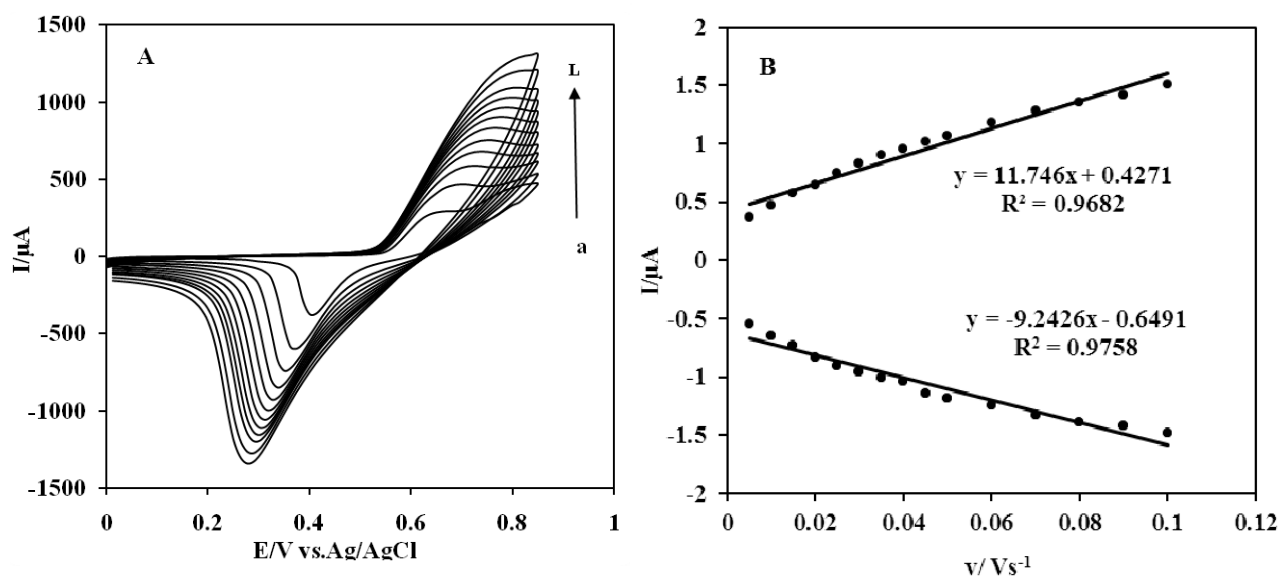


Fig. 2. (A) Cyclic voltammograms of Ni/Al-LDH/NMCP electrode in $0.1 \text{ mol L}^{-1} \text{ NaOH}$ at various potential scan rates: (a) 5, (b) 10, (c) 15, (d) 20, (e) 30, (f) 40, (g) 50, (h) 60, (i) 70, (j) 80, (k) 90 and (l) 100 mV s^{-1} . (B) The dependency of anodic and cathodic peak currents vs. scan rate

The Ni/Al-LDH/NMCP electrode was used for electrocatalytic oxidation of methanol. Fig. 3 presents the CVs of 0.05 mol L^{-1} methanol at (a) bare carbon paste electrode and (b) at Ni/Al-LDH/NMCP electrode at $0.1 \text{ mol L}^{-1} \text{ NaOH}$ solution. At the bare electrode, no anodic current due to the oxidation of methanol is observed but for Ni/Al-LDH/NMCP electrode a large anodic peak is observed. It was found that in comparison to bare carbon paste electrode, electrochemical behavior of methanol was greatly improved at Ni/Al-LDH/NMCP electrode, indicating that the anodic oxidation of methanol could be catalyzed at Ni/Al-LDH/NMCP electrode.

As has been reported in the literature [35–39], this behavior is typical of that expected for mediated oxidation of methanol as follows:



The relative decrease of the cathodic peak height in presence of methanol is attributed to the partial consumption of nickel oxyhydroxide species for the methanol oxidation with the formation of nickel hydroxide in accordance of reaction (2). This indicates clearly that the applied modifier in this process participates directly in the electrocatalytic oxidation of methanol.

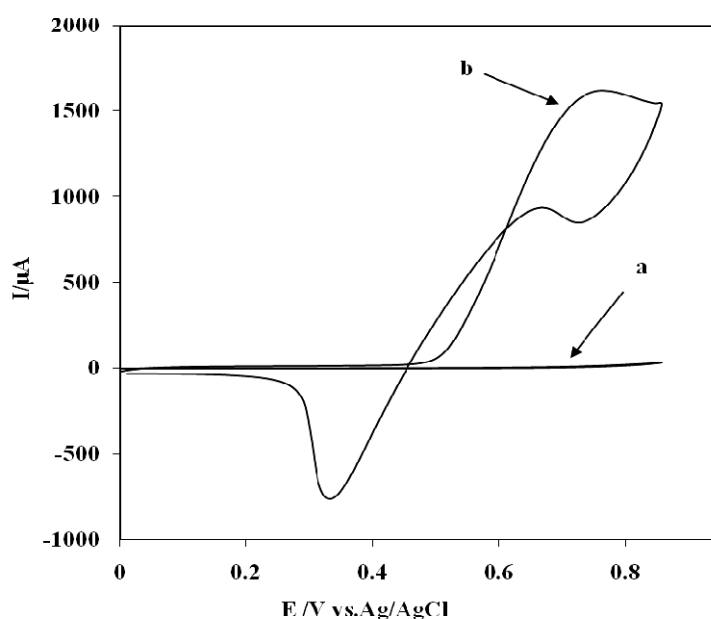


Fig. 3. Cyclic voltammograms of bare carbon paste (a) and Ni/Al-LDH/NMCP (b) electrode in 0.1 mol L^{-1} NaOH containing 0.05 mol L^{-1} methanol

It is generally agreed that the Ni-based catalysts such as nickel oxides and its complexes in a basic aqueous medium can catalyze methanol oxidation through an overall four electron process for producing format anion [27].



The effect of the modifier percentage (Ni/Al-LDH nanoparticles) on the intensity of methanol oxidation peak current was examined. The highest peak current for the Ni/Al-LDH/NMCP electrode was obtained when the content of the modifier was 25% in the paste. Of course, in concentrations more than 25%, a slight decrease in the

current was observed which could be attributed to reduction of the electrode surface conductivity. With all these results taken into account, carbon paste having 25% Ni/Al-LDH nanoparticles, 50% graphite and 25% mineral oil was used for later studies.

Here we present the effect of NaOH concentration on methanol oxidation at Ni/Al-LDH/NMCP electrode in Fig. 4. It can be seen that with an increase in OH^- concentration the peak current of methanol oxidation increase first and then begin to decrease remarkably at a NaOH concentration of 0.1 mol L^{-1} . The results indicate that the OH^- ion participates in the oxidation of methanol and may also be adverse to the oxidation of methanol for the competitive adsorption on the active sites to methanol. However, at high OH^- concentration ($>0.1 \text{ mol L}^{-1}$), the currents mainly come from the redox of Ni(III)/Ni(II) couple, because of the competitive adsorption on the active sites caused by OH^- . To obtain high oxidation current at lower oxidation potential, 0.1 mol L^{-1} NaOH was chosen as support electrolyte.

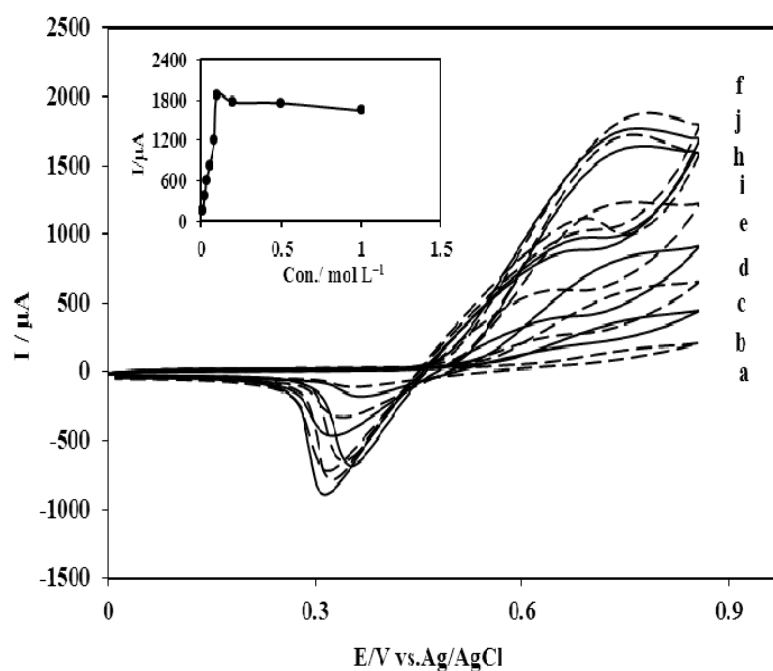


Fig. 4. Cyclic voltammograms of Ni/Al-LDH/NMCP electrode in 0.05 mol L^{-1} methanol containing different concentrations of NaOH at the scan rate of 50 mV s^{-1} . The NaOH concentration is (a) 0.01, (b) 0.02, (c) 0.03, (d) 0.05, (e) 0.08, (f) 0.1, (g) 0.2, (h) 0.5, and (i) 1.0 mol L^{-1} . The inset displays the peak currents vs. NaOH concentration

Fig. 5A shows the cyclic voltammograms of Ni/Al-LDH/NMCP electrode in 0.1 mol L^{-1} NaOH solution containing 0.05 mol L^{-1} methanol at different scan rates. The obtained results show that the catalytic effect of the mediator appeared at all testing scan rate. It can also be noted from this figure that, with an increasing scan rate, the peak potential for the catalytic oxidation of the methanol shifts to more positive potentials, suggesting a kinetic

limitation in the reaction between the redox sites of the modifier and the methanol. However, the peak current for the anodic oxidation of the methanol is proportional to the scan rate at high scan rates (Fig. 5B); which is an indication of an adsorption-controlled reaction. Also, plotting the current function against the potential sweep rate (Fig. 6) revealed negative slope confirming the electrocatalytic nature of the process.

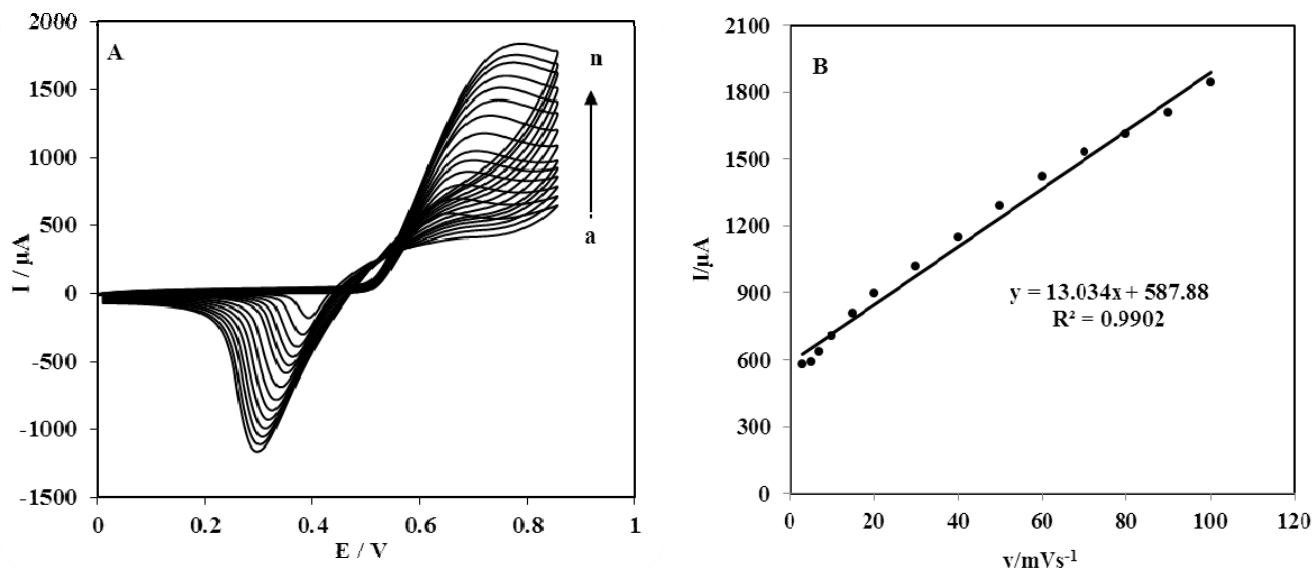


Fig. 5. (A) Cyclic voltammograms of Ni/Al-LDH/NMCP electrode in 0.1 mol L^{-1} NaOH containing 0.050 mol L^{-1} of methanol at various potential scan rates (from inner to outer) $3\text{-}100 \text{ mV s}^{-1}$. (B) Plot of I_p vs. v

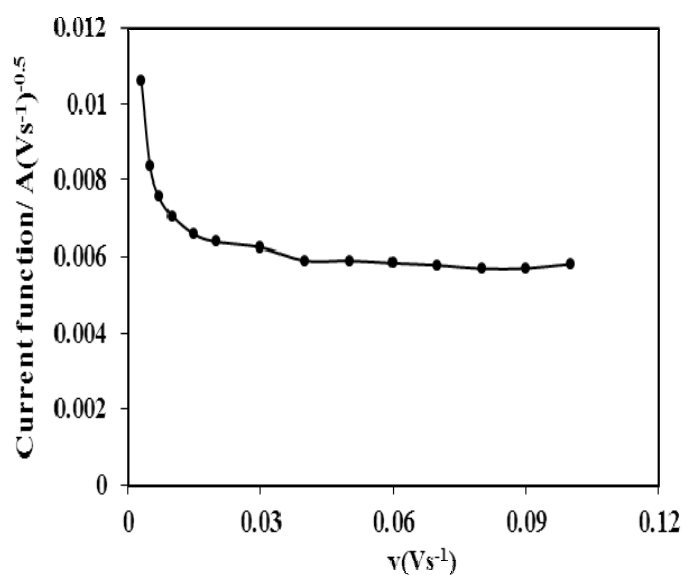


Fig. 6. Current function vs. v for 0.1 mol L^{-1} NaOH solution in the presence of 0.050 mol L^{-1} methanol

To obtain information on the rate-determining step, a Tafel plot was drawn (Fig. 7), derived from data of the rising part of the current–voltage curve at a low scan rate of 5 mV s^{-1} . A slope of $90.6 \text{ mV decade}^{-1}$ is obtained indicating the one-electron transfer to be rate limiting assuming an anodic electron-transfer coefficient of $\alpha = 0.65$.

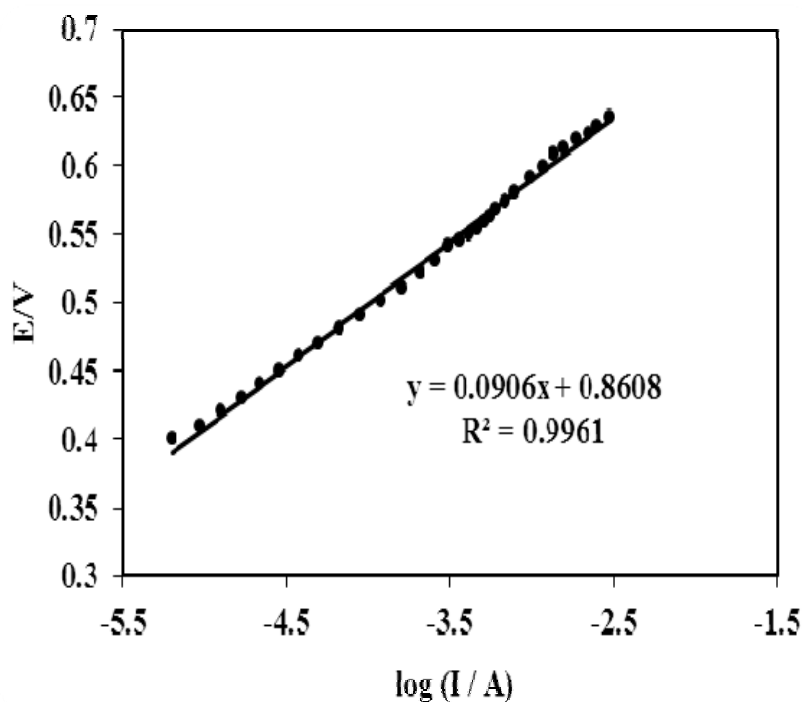


Fig. 7. Tafel plot derived from the rising part of voltammogram recorded at a scan rate 5 mV s^{-1}

The exchange current density (j_0) evaluated from Tafel plots is $7.55 \times 10^{-7} \text{ Acm}^{-2}$. The Tafel slope, b , can be obtained by another method. The peak potential, E_p , is proportional to $\log v$ as can be seen in Fig. 8. The slope of the plot of E_p vs. $\log v$ is $\partial E_p / \partial(\log v) = 47.916 \text{ mV decade}^{-1}$. The Tafel slope may be estimated according to the equation for the totally irreversible diffusion-controlled process [40]:

$$E_p = \frac{b}{2} \log v + \text{constant} \quad (2)$$

So, based on Eq. (2) $b = 95.832$. This result is close to that obtained from the polarization measurement. This slope indicates a one electron transfer to be rate limiting, assuming a transfer coefficient α of 0.62.

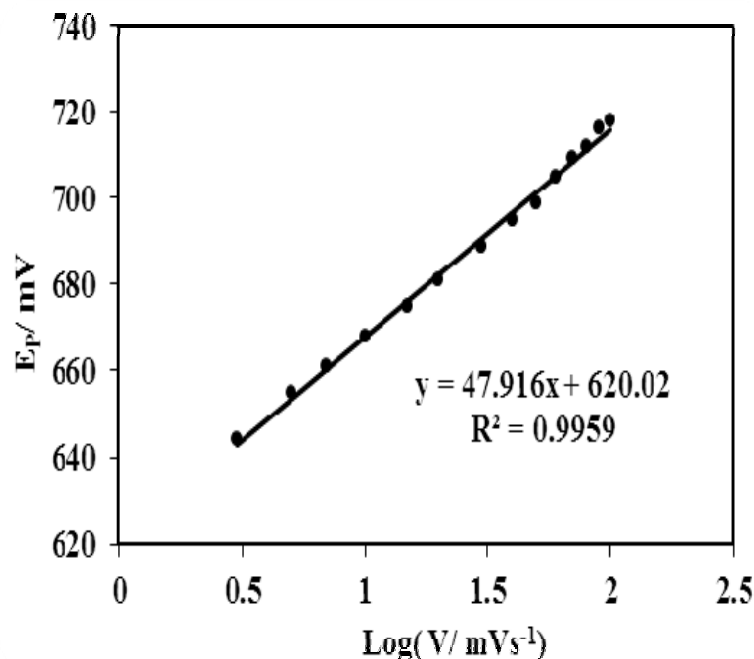


Fig. 8. Plot of E_p vs. $\log v$

Fig. 9 shows the effect of methanol concentration on the cyclic voltammograms of the Ni/Al-LDH/NMCP electrode. As can be seen from Fig. 9, the height of the anodic peak increases with increasing methanol concentration. The calibration curve obtained from these voltammograms is shown as the inset of this figure. There is a good linear relationship between the oxidation peak current and the methanol concentration in the range of 0.01 to 0.1 mol L⁻¹.

Chronoamperometry (CA) is also used to investigate the electro-oxidation of methanol on Ni/Al-LDH/NMCP electrode. Chronoamperograms of Ni/Al-LDH/NMCP electrode in the absence (curve a) and presence (Curves b–f) of methanol in 0.1 mol L⁻¹ NaOH at the oxidation potential of 750 mV vs. Ag/AgCl is presented in Fig. 10A. The inset of Fig. 10A shows plots of currents sampled at fixed time as a function of methanol concentration. The response is linearly proportional to the concentration of methanol in the range of 0.01–0.05 mol L⁻¹. Plotting of the net current with respect to the mines square roots of time presents a linear dependency (Fig. 10B). This indicates that the transient current must be controlled by a diffusion process. The transient current is due to catalytic oxidation of methanol and the current increases as the methanol concentration is raised. No significant cathodic current is observed when the electrolysis potential is stepped to 0 V vs. Ag/AgCl indicating the irreversible nature of the oxidation of methanol. CA results can also be employed to evaluate the catalytic rate constant (k) for the electrode reaction according to [41]:

$$\frac{I_{\text{catal}}}{I_d} = \lambda^{1/2} \pi^{1/2} = \pi^{1/2} (kCt)^{1/2} \quad (3)$$

where I_{cat} is the catalytic current, I_d is the limiting current in the absence of methanol and $\lambda = kCt$ (k , C and t are the catalytic rate constant, bulk concentration of methanol and the elapsed time, respectively). Based on the slope of the I_{catal}/I_d vs. $t^{1/2}$ plot, the value of k for 0.05 mol L^{-1} methanol was calculated to be $5.4 \times 10^4 \text{ cm}^3 \text{ mol}^{-1} \text{ s}^{-1}$ (Fig. 10C).

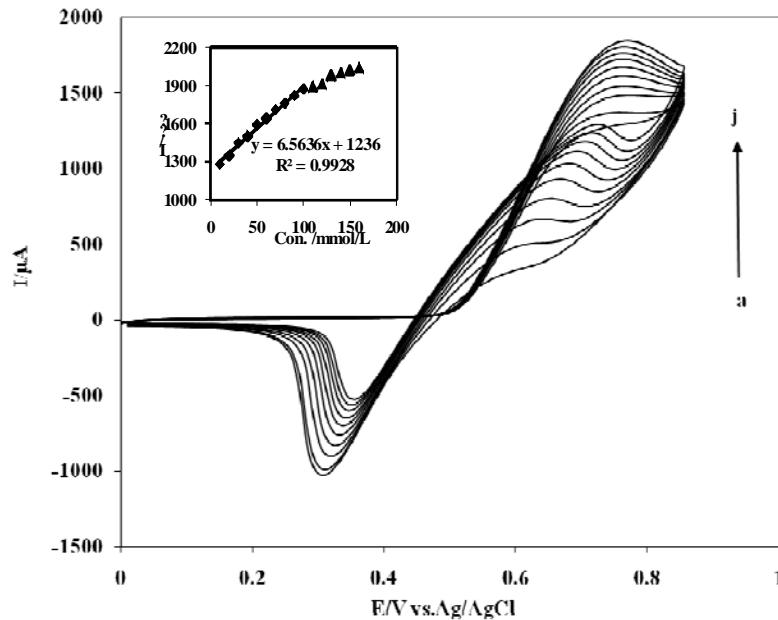


Fig. 9. Cyclic voltammograms of different concentrations of methanol at Ni/Al-LDH/NMCP electrode in 0.1 mol L^{-1} NaOH at a scan rate of 50 mV s^{-1} . Concentrations of methanol from (a) to (j) are $0.01, 0.02, 0.03, 0.04, 0.05, 0.06, 0.07, 0.08, 0.09$ and 0.1 mol L^{-1} , respectively

Fig. 11 indicates pseudo-steady-state current–potential curves recorded for the electrocatalytic oxidation of methanol. Typical S-shape plots have been obtained.

The rate law for the Ni (III) mediated oxidation of methanol is derived through:

$$v_1 = k_1 \Gamma \theta_{II} - k_{-1} \Gamma \theta_{III} \quad (4)$$

$$v_2 = k_2 \Gamma \theta_{III} C_m \quad (5)$$

Where Γ is the total number of adsorption sites per unit area of the electrode surface's represent the fractional surface coverage of nickel of different valence states and C_m is the bulk concentration of methanol. With only the 2 and 3 valence states of nickel prevailing one has:

$$\theta_{II} + \theta_{III} = 1 \quad (6)$$

And the rates of changes of their surface coverage as well as that of the intermediate compounds are:

$$\frac{d\theta_{II}}{dt} = -\frac{d\theta_{III}}{dt} = -k_1\theta_{II} + k_{-1}\theta_{III} + k_2\theta_{III}C_m + k_3\theta_{III}C_i \quad (7)$$

$$\frac{dC_i}{dt} = k_2\theta_{III}C_m - k_3\theta_{III}C_i \quad (8)$$

Where C_i is the concentration of the intermediate. Assuming that the steady state dominates:

$$\frac{d\theta_{II}}{dt} = -\frac{d\theta_{III}}{dt} = 0 \quad (9)$$

$$\frac{dC_i}{dt} = 0 \quad (10)$$

One arrives at the values if the coverage:

$$\theta_{II} = \left(\frac{k_{-1} + 2k_2C_m}{k_1 + k_{-1} + 2k_2C_m} \right) \quad (11)$$

$$\theta_{III} = \left(\frac{k_1}{k_1 + k_{-1} + 2k_2C_m} \right) \quad (12)$$

And subsequently:

$$v_1 = \left(\frac{2k_1\Gamma k_2C_m}{k_1 + k_{-1} + 2k_2C_m} \right) \quad (13)$$

On the basis of this rate equation the faradic current will be:

$$i_f = \left(\frac{2FAk_1\Gamma k_2C_m}{k_1 + k_{-1} + 2k_2C_m} \right) \quad (14)$$

Where A is the surface area of the electrode and the rate constants k_1 and k_{-1} are obviously potential dependent and are of the forms:

$$k_1(E) = k_1^0 \exp\left[\frac{\alpha nFE}{RT}\right] \quad (15)$$

$$k_{-1}(E) = k_{-1}^0 \exp\left[\frac{(\alpha - 1)nFE}{RT}\right] \quad (16)$$

Where k^0 's are the chemical rate constants measured at $E/\text{Ag}/\text{AgCl}=0$ with α being the anodic transfer coefficient and other parameters have their usual meanings [42]. Eq. (14) is well suited for the calculation of rate constants and the validity test of the kinetics and mechanism of the oxidation process.

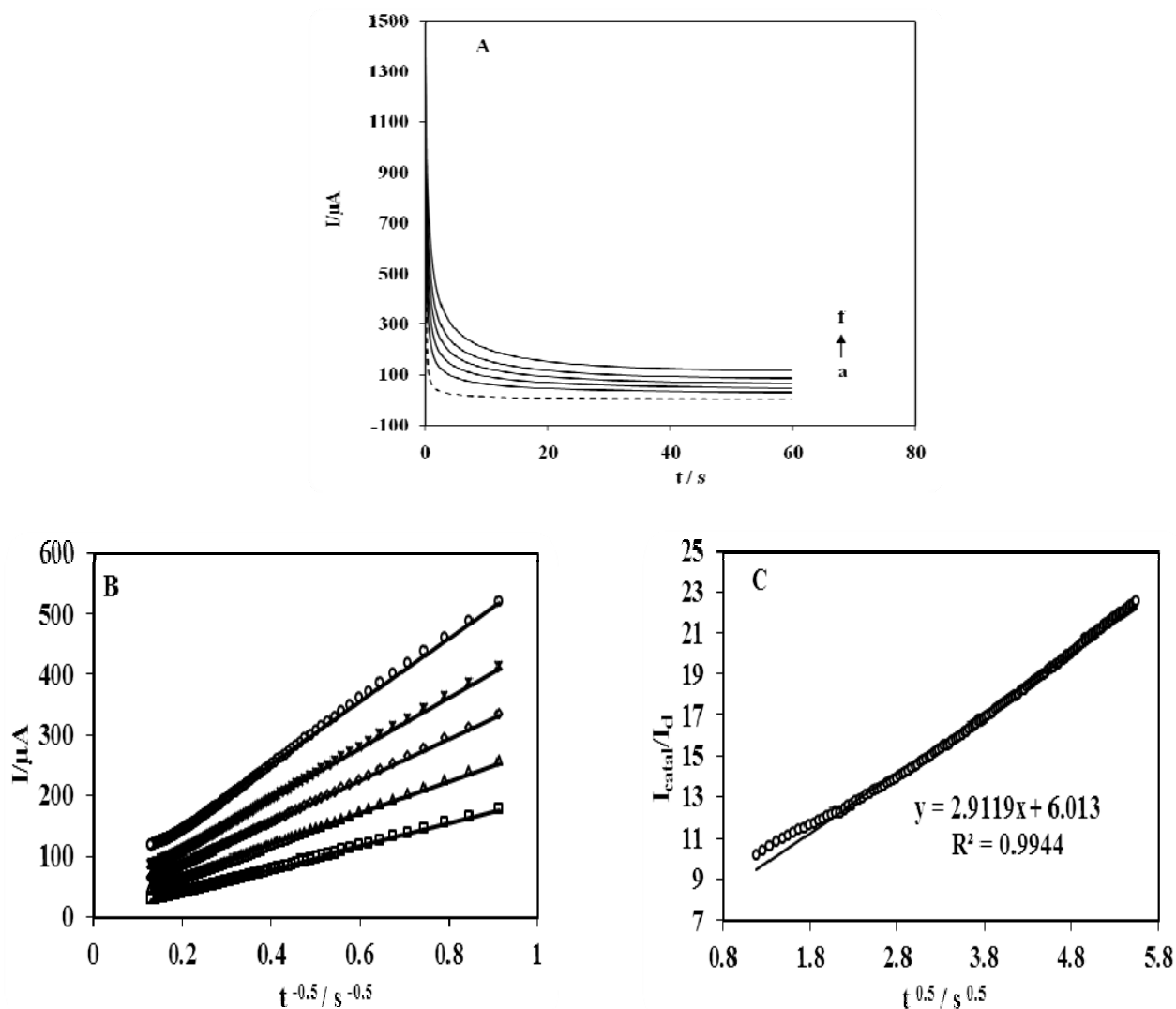


Fig. 10. (A) Chronoamperograms of Ni-Al LDH/MCP electrode in 0.1 M NaOH containing different concentrations of methanol: 0.0, 0.01, 0.02, 0.03, 0.04 and 0.05 mol L⁻¹, from (a) to (f), respectively. Potential steps were 0.75 and 0.0 V, respectively. (B) Dependency of transient current on $t^{-1/2}$. (C) Dependency of I_{cat}/I_d on $t^{1/2}$ derived from CAs of (a) and (f) in panel (A)

The pseudo-steady state polarization curves of the electro-oxidation of methanol on Ni-Al LDH modified carbon past electrode at a number of methanol concentrations are presented in Fig. 11. The rotation rate of the electrode is maintained at 3000 rpm to avoid the interference of the mass transfer in the kinetics measurements. The oxidation process was found to begin at nearly 550 mV vs. Ag/AgCl and to reach a plateau at 670 mV vs. Ag/AgCl while the oxygen evolution starts at still higher potentials. In the course of reaction the coverage of Ni (III) increases and reaches a saturation (steady state) level and the oxidation current follows accordingly. At potentials as high as 740 mV vs. Ag/AgCl the decomposition (oxidation) of solvent interferes and the plateau region become ill defined.

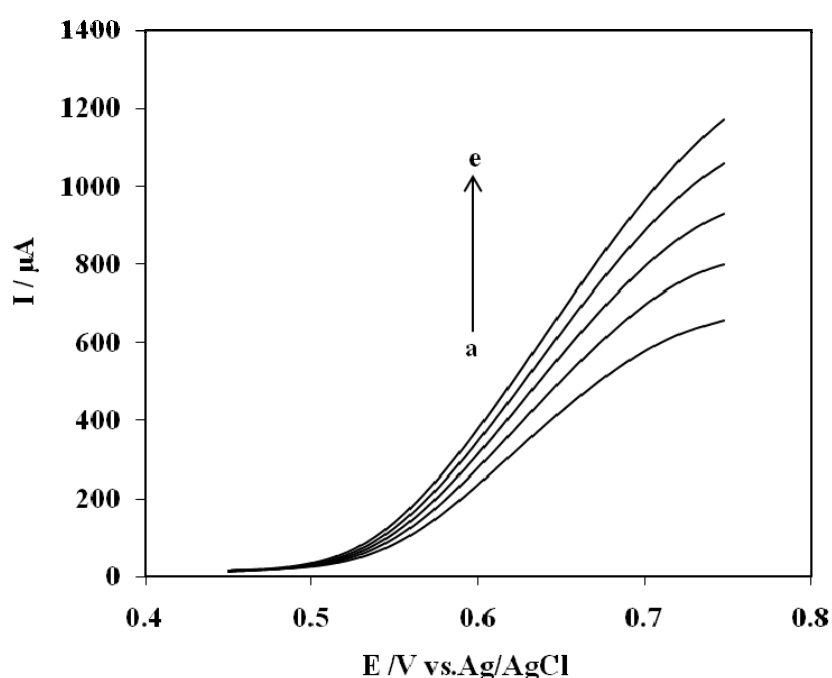


Fig. 11. Pseudo-steady state polarization curves of Ni-Al LDH/NMCP electrode obtained in 0.03 (a), 0.004 (b), 0.05 (c), 0.06 (d) and 0.1 (e) mol L⁻¹ methanol respectively. The potential sweep rate is 5 mVs⁻¹

According to Eq. (17) the plots of the inverse of current against the inverse of methanol concentration should be linear:

$$i_f^{-1} = (FAk_1\Gamma)^{-1} + \left[\frac{k_1 + k_{-1}}{2FAk_1k_2\Gamma} \right] c_m^{-1} \quad (17)$$

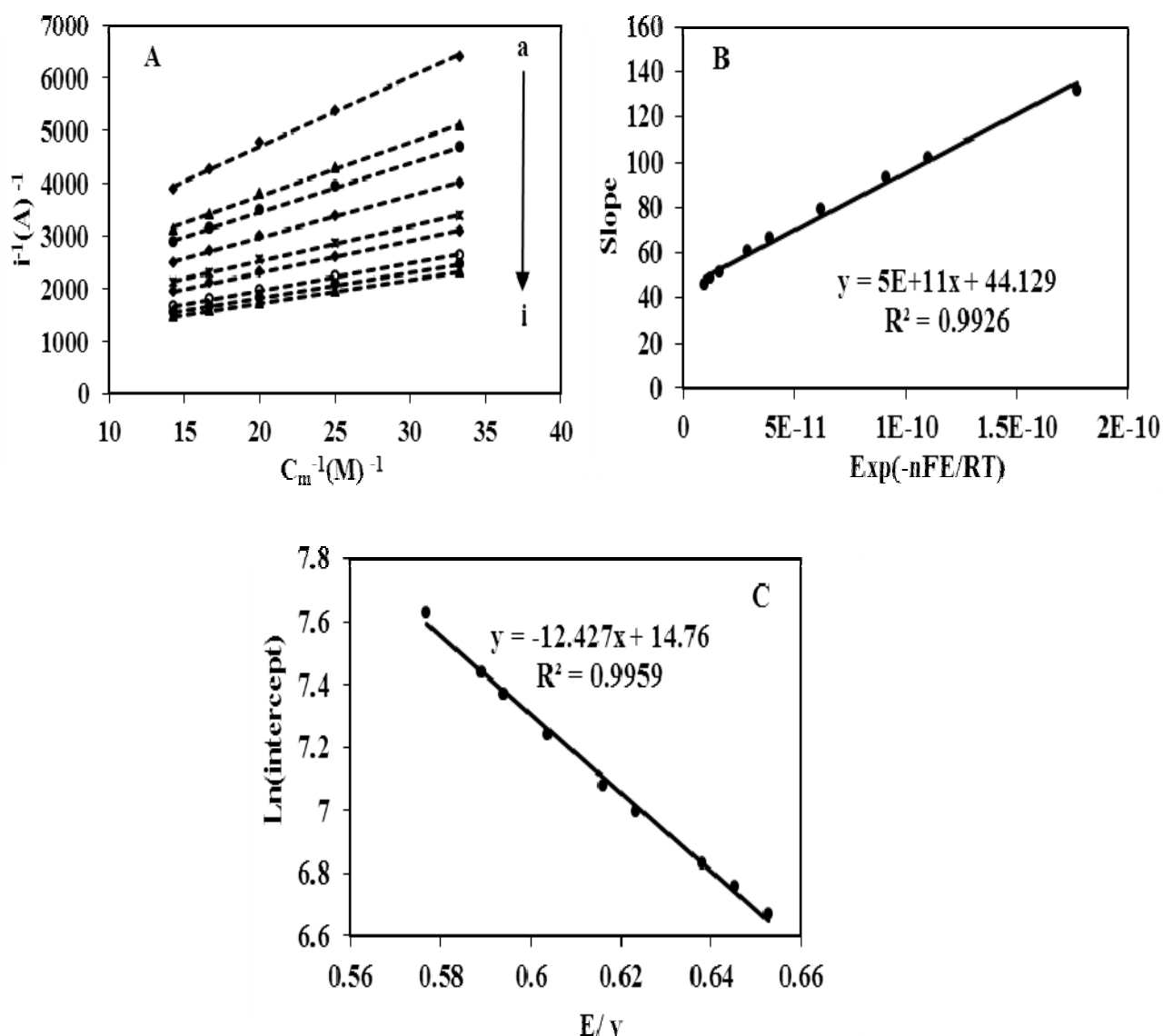


Fig. 12. (A) Plot of i^{-1} (from polarization curves in Fig. 11. against C_m^{-1} at various potentials: (a) 576; (b) 589; (c) 594; (d) 602; (e) 616; (f) 623; (g) 638; (h) 645 and (i) 652 mV/Ag, AgCl as curves (a–i). (B) Plot of the slopes (of curves in 12A) vs. $\text{exp}(-nFE/RT)$. (C) Plot of the $\text{Ln}(\text{intercepts})$ (of curves in 12A) vs. applied potential

Fig. 12A presents the i^{-1} vs. C_m^{-1} dependencies where straight lines at various potentials have been obtained. Both the intercepts and slopes of the straight lines appearing in this figure were potential dependent. The slopes are plotted against $\text{exp}(-nFE/RT)$ with $n=1$ and the graph is presented in Fig. 12A Using this graph along with Eq. (17) reveals that the rate constant of reaction, $k_2\Gamma$ and the ratio of k_0^{-1}/k_0^1 are $9.3 \times 10^{-10} \text{ cm s}^{-1}$ and 1.13×10^{10} respectively. Fig. 12C presents the variation of the intercepts of the lines in Fig. 12A with the

applied potential in a semi-log scale. Using this graph and Eq. (17) the magnitudes of $k_0\Gamma$ and the anodic transfer coefficient of $3.2 \times 10^{-11} \text{ mol s}^{-1} \text{ cm}^{-2}$ and 0.36 have been obtained.

4. CONCLUSION

Ni/Al-LDH nanoparticles were employed as a modifier for preparation of a new carbon paste electrode. The modified electrode has very good electrocatalytic activity. The electrochemical behavior of methanol was greatly improved at the surface of Ni/Al-LDH/NMCP electrode. The charge transfer coefficient and the number of electrons involved in the rate-determining step were calculated. High stability, good reproducibility, rapid response, easy surface regeneration and fabrication are the important characteristics of the proposed electrode.

REFERENCES

- [1] J. B. Raoof, N. Azizi, R. Ojani, S. Ghodrati, M. Abrishamkar, and F. Cheken, *Int. J. Hydrogen Energ.* 36 (2011) 13295.
- [2] Z. Wang, G. Gao, H. Zhu, Z. Sun, H. Liu, and X. Zhao, *Int. J. Hydrogen Energ.* 34 (2009) 9334.
- [3] T. Iwasita, *Electrochim. Acta* 47 (2002) 3663.
- [4] I. Danaee, M. Jafariana, F. Forouzandeha, F. Gobalb, and M. G. Mahjania, *Int. J. Hydrogen Energ.* 33 (2009) 4367.
- [5] H. Nonaka, and Y. Matsumura, *J. Electroanal. Chem.* 520 (2002) 101.
- [6] C. L. Green, and A. Kucernak, *J. Phys. Chem.* 106 B (2002) 1036.
- [7] A. S. Arico, Z. Poltarzewski, H. Kim, A. Morana, N. Giordano, and Vantonucci, *J. Power Sources* 55 (1995) 159.
- [8] M. Jafarian, M. G. Mahjani, H. Heli, F. Gobal, H. Khajesharifi, and M. H. Hamed, *Electrochim. Acta* 48 (2003) 3423.
- [9] S. M. Golabi, and A. N. Golikand, *Electroanalysis* 15 (2003) 278.
- [10] F. E. Jones, S. B. Milen, B. Gurau, E. S. Smotkin, S. R. Stock, and C. M. Lukehart, *J. Nanosci. Nanotechnol.* 2 (2002) 81.
- [11] J. Luo, M. M. Maye, Y. Lou, L. Han, M. Hepel, and C. J. Zhong, *Catal. Today* 77 (2002) 127.
- [12] A. A. El-Shafei, *J. Electroanal. Chem.* 471 (1999) 89.
- [13] M. S. Kim, T. S. Hwang, and K. B. Kim, *J. Electrochem. Soc.* 144 (1997) 151.
- [14] M. A. Abdel Rahim, R. M. Abdel Hameed, and M. W. Khalil, *J. Power Sources* 134 (2004) 160.

- [15] Z. Borkowska, A. Tymosiak-Zielinska, and G. Shul, *Electrochim. Acta* 49 (2004) 1209.
- [16] B. Guo, S. Zhao, G. Han, and L. Zhang, *Electrochim. Acta* 53 (2008) 5174.
- [17] C. Xu, Z. Tian, P. Shen, and S. P. Jiang, *Electrochim. Acta* 53 (2008) 2610.
- [18] E. Antolini, and E. R. Gonzalez, *J. Power Sources* 195 (2010) 3431.
- [19] I. G. Casella, T. R. I. Cataldi, A. M. Salvi, and E. Desimoni, *Anal. Chem.* 65 (1993) 3143.
- [20] C. Xu, Y. Hu, J. Rong, S. P. Jiang, and Y. Liu, *Electrochem. Commun.* 9 (2007) 2009.
- [21] Y. Zhao, Y. E, L. Fan, Y. Qiu, and S. Yang, *Electrochim. Acta* 52 (2007) 5873.
- [22] I. Danaee, M. Jafarian, F. Forouzandeh, F. Gobal, and M. G. Mahjani, *Int. J. Hydrogen Energ.* 33 (2008) 4367.
- [23] I. Danaee, M. Jafarian, A. Mirzapoor, F. Gobal, and M. G. Mahjani, *Electrochim. Acta* 55 (2010) 2093.
- [24] M. Jafarian, M. G. Mahjani, H. Helia, F. Gobal, and M. Heydarpoor, *Electrochem. Commun.* 5 (2003) 184.
- [25] A. N. Golikand, S. Shahrokhian, M. Asgari, M.G. Maragheh, L. Irannejad, and A. Khanchi, *J. Power Sources* 144 (2005) 21.
- [26] M. A. Abdel Rahim, B. Hanaa, R. M. Hassan, and R. M. Abdel Hamid, *J. Power Sources* 154 (2006) 59.
- [27] W. S. Cardoso, V. L. N. Dias, W. M. Costa, I. Araujo Rodrigues, E. P. Marques, A. G. Sousa, J. Boaventura, C. W. B. Bezerra, C. Song, H. Liu, J. Zhang, and A. L. B. Marques, *J. Appl. Electrochem.* 39 (2009) 55.
- [28] S. M. Golabi, and A. Nozadb, *Electroanalysis* 16 (2004) 199.
- [29] Z. Zhu, L. Qu, Y. Guo, Y. Zeng, W. Sun, and X. Huang, *Sens. Actuators B* 151 (2010) 146.
- [30] L. Guadagnini, A. Mignani, E. Scavetta, and D. Tonelli, *Electrochim. Acta* 55 (2010) 1217.
- [31] B. Ballarin, R. Seeber, D. Tonelli, and A. Vaccari, *J. Electroanal. Chem.* 463 (1999) 123.
- [32] Y. Wang, D. Zhang, M. Tang, S. Xu, and M. Li, *Electrochim. Acta* 55 (2010) 4045.
- [33] V. Prevot, N. Caperaa, C. Taviot-Gue'ho, and C. Forano, *Cryst. Growth. Des.* 9 (2009) 3646
- [34] G. Karim-Nezhad, M. Hasanzadeh, L. A. Saghatforoush, N. Shadjou, S. Earshad, and B. Khalilzadeh, *J. Braz. Chem. Soc.* 20 (2009) 141.
- [35] A. N. Golikand, M. Asgari, M. G. Maragheh, and S. Shahrokhian, *J. Electroanal. Chem.* 588 (2006) 155.
- [36] J. B. Raoof, R. Ojani, and S. R. Hosseini, *J. Power Sources* 196 (2011) 1855.

- [37] S. J. Liu, *Electrochim. Acta* 49 (2004) 3235.
- [38] A. N. Golikand, S. Shahrokhian, M. Asgari, M. G. Maragheh, L. Irannejad, and A. Khanchi, *J. Power Sources* 144 (2005) 21.
- [39] A. Ciszewski, G. Milczarek, B. Lewandowska, and K. Krutowski, *Electroanal.* 15 (2003) 518.
- [40] G. Karim-Nezhad, and P. Seyed Dorraji, *Electrochim. Acta* 55 (2010) 3414.
- [41] M. Hasanzadeh, G. Karim-Nezhad, N. Shadjou, B. Khalilzadeh, L. A. Saghatforoush, S. Earshad, and I. Kazeman, *Chin. J. Chem.* 27 (2009) 638.
- [42] M. Hasanzadeh, G. Karim-Nezhad, M. G. Mahjani, M. Jafarian, N. Shadjou, B. Khalilzadeh, and L. A. Saghatforoush, *Catal. Commun.* 10 (2008) 295.